

Proceedings of the 12th International Conference on
Computational Fluid Dynamics in the Oil & Gas,
Metallurgical and Process Industries

Progress in Applied CFD – CFD2017



SINTEF Proceedings

Editors:

Jan Erik Olsen and Stein Tore Johansen

Progress in Applied CFD – CFD2017

Proceedings of the 12th International Conference on Computational Fluid Dynamics
in the Oil & Gas, Metallurgical and Process Industries

SINTEF Academic Press

SINTEF Proceedings no 2

Editors: Jan Erik Olsen and Stein Tore Johansen

Progress in Applied CFD – CFD2017

Selected papers from 10th International Conference on Computational Fluid Dynamics in the Oil & Gas, Metallurgical and Process Industries

Key words:

CFD, Flow, Modelling

Cover, illustration: Arun Kamath

ISSN 2387-4295 (online)

ISBN 978-82-536-1544-8 (pdf)

© Copyright SINTEF Academic Press 2017

The material in this publication is covered by the provisions of the Norwegian Copyright Act. Without any special agreement with SINTEF Academic Press, any copying and making available of the material is only allowed to the extent that this is permitted by law or allowed through an agreement with Kopinor, the Reproduction Rights Organisation for Norway. Any use contrary to legislation or an agreement may lead to a liability for damages and confiscation, and may be punished by fines or imprisonment

SINTEF Academic Press

Address: Forskningsveien 3 B
 PO Box 124 Blindern
 N-0314 OSLO

Tel: +47 73 59 30 00

Fax: +47 22 96 55 08

www.sintef.no/byggforsk

www.sintefbok.no

SINTEF Proceedings

SINTEF Proceedings is a serial publication for peer-reviewed conference proceedings on a variety of scientific topics.

The processes of peer-reviewing of papers published in SINTEF Proceedings are administered by the conference organizers and proceedings editors. Detailed procedures will vary according to custom and practice in each scientific community.

PREFACE

This book contains all manuscripts approved by the reviewers and the organizing committee of the 12th International Conference on Computational Fluid Dynamics in the Oil & Gas, Metallurgical and Process Industries. The conference was hosted by SINTEF in Trondheim in May/June 2017 and is also known as CFD2017 for short. The conference series was initiated by CSIRO and Phil Schwarz in 1997. So far the conference has been alternating between CSIRO in Melbourne and SINTEF in Trondheim. The conferences focuses on the application of CFD in the oil and gas industries, metal production, mineral processing, power generation, chemicals and other process industries. In addition pragmatic modelling concepts and bio-mechanical applications have become an important part of the conference. The papers in this book demonstrate the current progress in applied CFD.

The conference papers undergo a review process involving two experts. Only papers accepted by the reviewers are included in the proceedings. 108 contributions were presented at the conference together with six keynote presentations. A majority of these contributions are presented by their manuscript in this collection (a few were granted to present without an accompanying manuscript).

The organizing committee would like to thank everyone who has helped with review of manuscripts, all those who helped to promote the conference and all authors who have submitted scientific contributions. We are also grateful for the support from the conference sponsors: ANSYS, SFI Metal Production and NanoSim.

Stein Tore Johansen & Jan Erik Olsen



Organizing committee:

Conference chairman: Prof. Stein Tore Johansen

Conference coordinator: Dr. Jan Erik Olsen

Dr. Bernhard Müller

Dr. Sigrid Karstad Dahl

Dr. Shahriar Amini

Dr. Ernst Meese

Dr. Josip Zoric

Dr. Jannike Solsvik

Dr. Peter Witt

Scientific committee:

Stein Tore Johansen, SINTEF/NTNU

Bernhard Müller, NTNU

Phil Schwarz, CSIRO

Akio Tomiyama, Kobe University

Hans Kuipers, Eindhoven University of Technology

Jinghai Li, Chinese Academy of Science

Markus Braun, Ansys

Simon Lo, CD-adapco

Patrick Segers, Universiteit Gent

Jiyuan Tu, RMIT

Jos Derksen, University of Aberdeen

Dmitry Eskin, Schlumberger-Doll Research

Pär Jönsson, KTH

Stefan Pirker, Johannes Kepler University

Josip Zoric, SINTEF

CONTENTS

PRAGMATIC MODELLING	9
On pragmatism in industrial modeling. Part III: Application to operational drilling	11
CFD modeling of dynamic emulsion stability	23
Modelling of interaction between turbines and terrain wakes using pragmatic approach	29
FLUIDIZED BED	37
Simulation of chemical looping combustion process in a double looping fluidized bed reactor with cu-based oxygen carriers.....	39
Extremely fast simulations of heat transfer in fluidized beds.....	47
Mass transfer phenomena in fluidized beds with horizontally immersed membranes	53
A Two-Fluid model study of hydrogen production via water gas shift in fluidized bed membrane reactors	63
Effect of lift force on dense gas-fluidized beds of non-spherical particles	71
Experimental and numerical investigation of a bubbling dense gas-solid fluidized bed	81
Direct numerical simulation of the effective drag in gas-liquid-solid systems	89
A Lagrangian-Eulerian hybrid model for the simulation of direct reduction of iron ore in fluidized beds.....	97
High temperature fluidization - influence of inter-particle forces on fluidization behavior	107
Verification of filtered two fluid models for reactive gas-solid flows	115
BIOMECHANICS.....	123
A computational framework involving CFD and data mining tools for analyzing disease in carotid artery	125
Investigating the numerical parameter space for a stenosed patient-specific internal carotid artery model.....	133
Velocity profiles in a 2D model of the left ventricular outflow tract, pathological case study using PIV and CFD modeling.....	139
Oscillatory flow and mass transport in a coronary artery.....	147
Patient specific numerical simulation of flow in the human upper airways for assessing the effect of nasal surgery.....	153
CFD simulations of turbulent flow in the human upper airways	163
OIL & GAS APPLICATIONS	169
Estimation of flow rates and parameters in two-phase stratified and slug flow by an ensemble Kalman filter	171
Direct numerical simulation of proppant transport in a narrow channel for hydraulic fracturing application	179
Multiphase direct numerical simulations (DNS) of oil-water flows through homogeneous porous rocks	185
CFD erosion modelling of blind tees	191
Shape factors inclusion in a one-dimensional, transient two-fluid model for stratified and slug flow simulations in pipes	201
Gas-liquid two-phase flow behavior in terrain-inclined pipelines for wet natural gas transportation	207

NUMERICS, METHODS & CODE DEVELOPMENT	213
Innovative computing for industrially-relevant multiphase flows	215
Development of GPU parallel multiphase flow solver for turbulent slurry flows in cyclone.....	223
Immersed boundary method for the compressible Navier–Stokes equations using high order summation-by-parts difference operators	233
Direct numerical simulation of coupled heat and mass transfer in fluid-solid systems	243
A simulation concept for generic simulation of multi-material flow, using staggered Cartesian grids.....	253
A cartesian cut-cell method, based on formal volume averaging of mass, momentum equations.....	265
SOFT: a framework for semantic interoperability of scientific software	273
 POPULATION BALANCE	 279
Combined multifluid-population balance method for polydisperse multiphase flows	281
A multifluid-PBE model for a slurry bubble column with bubble size dependent velocity, weight fractions and temperature.....	285
CFD simulation of the droplet size distribution of liquid-liquid emulsions in stirred tank reactors	295
Towards a CFD model for boiling flows: validation of QMOM predictions with TOPFLOW experiments	301
Numerical simulations of turbulent liquid-liquid dispersions with quadrature-based moment methods.....	309
Simulation of dispersion of immiscible fluids in a turbulent couette flow	317
Simulation of gas-liquid flows in separators - a Lagrangian approach.....	325
CFD modelling to predict mass transfer in pulsed sieve plate extraction columns	335
 BREAKUP & COALESCENCE	 343
Experimental and numerical study on single droplet breakage in turbulent flow	345
Improved collision modelling for liquid metal droplets in a copper slag cleaning process	355
Modelling of bubble dynamics in slag during its hot stage engineering.....	365
Controlled coalescence with local front reconstruction method	373
 BUBBLY FLOWS	 381
Modelling of fluid dynamics, mass transfer and chemical reaction in bubbly flows	383
Stochastic DSMC model for large scale dense bubbly flows.....	391
On the surfacing mechanism of bubble plumes from subsea gas release.....	399
Bubble generated turbulence in two fluid simulation of bubbly flow	405
 HEAT TRANSFER	 413
CFD-simulation of boiling in a heated pipe including flow pattern transitions using a multi-field concept	415
The pear-shaped fate of an ice melting front	423
Flow dynamics studies for flexible operation of continuous casters (flow flex cc).....	431
An Euler-Euler model for gas-liquid flows in a coil wound heat exchanger.....	441
 NON-NEWTONIAN FLOWS.....	 449
Viscoelastic flow simulations in disordered porous media	451
Tire rubber extrudate swell simulation and verification with experiments	459
Front-tracking simulations of bubbles rising in non-Newtonian fluids.....	469
A 2D sediment bed morphodynamics model for turbulent, non-Newtonian, particle-loaded flows.....	479

METALLURGICAL APPLICATIONS.....	491
Experimental modelling of metallurgical processes	493
State of the art: macroscopic modelling approaches for the description of multiphysics phenomena within the electroslag remelting process	499
LES-VOF simulation of turbulent interfacial flow in the continuous casting mold	507
CFD-DEM modelling of blast furnace tapping	515
Multiphase flow modelling of furnace tapholes	521
Numerical predictions of the shape and size of the raceway zone in a blast furnace.....	531
Modelling and measurements in the aluminium industry - Where are the obstacles?	541
Modelling of chemical reactions in metallurgical processes.....	549
Using CFD analysis to optimise top submerged lance furnace geometries	555
Numerical analysis of the temperature distribution in a martensic stainless steel strip during hardening.....	565
Validation of a rapid slag viscosity measurement by CFD.....	575
Solidification modeling with user defined function in ANSYS Fluent.....	583
Cleaning of polycyclic aromatic hydrocarbons (PAH) obtained from ferroalloys plant.....	587
Granular flow described by fictitious fluids: a suitable methodology for process simulations	593
A multiscale numerical approach of the dripping slag in the coke bed zone of a pilot scale Si-Mn furnace.....	599
INDUSTRIAL APPLICATIONS	605
Use of CFD as a design tool for a phosphoric acid plant cooling pond	607
Numerical evaluation of co-firing solid recovered fuel with petroleum coke in a cement rotary kiln: Influence of fuel moisture	613
Experimental and CFD investigation of fractal distributor on a novel plate and frame ion-exchanger	621
COMBUSTION	631
CFD modeling of a commercial-size circle-draft biomass gasifier.....	633
Numerical study of coal particle gasification up to Reynolds numbers of 1000.....	641
Modelling combustion of pulverized coal and alternative carbon materials in the blast furnace raceway	647
Combustion chamber scaling for energy recovery from furnace process gas: waste to value	657
PACKED BED.....	665
Comparison of particle-resolved direct numerical simulation and 1D modelling of catalytic reactions in a packed bed	667
Numerical investigation of particle types influence on packed bed adsorber behaviour	675
CFD based study of dense medium drum separation processes	683
A multi-domain 1D particle-reactor model for packed bed reactor applications.....	689
SPECIES TRANSPORT & INTERFACES	699
Modelling and numerical simulation of surface active species transport - reaction in welding processes	701
Multiscale approach to fully resolved boundary layers using adaptive grids.....	709
Implementation, demonstration and validation of a user-defined wall function for direct precipitation fouling in Ansys Fluent.....	717

FREE SURFACE FLOW & WAVES	727
Unresolved CFD-DEM in environmental engineering: submarine slope stability and other applications.....	729
Influence of the upstream cylinder and wave breaking point on the breaking wave forces on the downstream cylinder	735
Recent developments for the computation of the necessary submergence of pump intakes with free surfaces	743
Parallel multiphase flow software for solving the Navier-Stokes equations	752
PARTICLE METHODS	759
A numerical approach to model aggregate restructuring in shear flow using DEM in Lattice-Boltzmann simulations	761
Adaptive coarse-graining for large-scale DEM simulations.....	773
Novel efficient hybrid-DEM collision integration scheme.....	779
Implementing the kinetic theory of granular flows into the Lagrangian dense discrete phase model.....	785
Importance of the different fluid forces on particle dispersion in fluid phase resonance mixers	791
Large scale modelling of bubble formation and growth in a supersaturated liquid.....	798
FUNDAMENTAL FLUID DYNAMICS	807
Flow past a yawed cylinder of finite length using a fictitious domain method	809
A numerical evaluation of the effect of the electro-magnetic force on bubble flow in aluminium smelting process.....	819
A DNS study of droplet spreading and penetration on a porous medium.....	825
From linear to nonlinear: Transient growth in confined magnetohydrodynamic flows.....	831

SOLIDIFICATION MODELING WITH USER DEFINED FUNCTION IN ANSYS FLUENT

Moritz EICKHOFF^{1*}, Antje RÜCKERT¹, Herbert PFEIFER¹

¹ RWTH Aachen University, Department for Industrial Furnaces and Heat Engineering, Kopernikusstr. 10, 52074 Aachen, GERMANY

* E-mail: eickhoff@iob.rwth-aachen.de

ABSTRACT

The modelling of solidification processes in combination with fluid flow is one main application of ANSYS Fluent. The solidification is modelled with the enthalpy porosity technique. Therefore the fluid flow is damped like a flow through a porous media of dendrites. In case of materials with large solidification ranges, like the nickel based superalloy 718, the adjustment possibilities of ANSYS Fluent are often not adequate. The program postulates a linear dependency between liquid fraction and temperature. To improve the simulation, the solidification was implemented by a user defined function (UDF). The principal modelling of fluid flow is based on the theory of ANSYS Fluent, but it is now possible to adjust the liquid fraction in fine temperature steps.

Keywords: Rheology, Interphases, Casting and solidification, Process metallurgy, Alloy 718.

NOMENCLATURE

Greek Symbols

ϵ	Turbulent dissipation rate, [-].
λ	Thermal conductivity, [W/(m K)].
μ_D	Dynamic viscosity, [kg/(m s)].
∇	Divergence operator, [-].
ρ	Density, [kg/m ³].
τ	Shear stress tensor, [N/m ²].

Latin Symbols

A_{mush}	Mushy zone constant, [kg/(m ³ s)].
e	Internal energy, [J].
f	Fraction, [-].
F	Force against fluid flow per volume, [N/m ³].
g	Gravity, [m/s ²].
k	Turbulent kinetic energy, [-].
K	Permeability, [m ²].
l	Small number, [-].
p	Pressure, [Pa].
Q_e	volumetric energy source, [J/m ³].
S	Momentum sink for turbulence, [kg/(m ³ s)].
v	Velocity, [m/s].
t	Time, [s].
T	Temperature, [K].

Sub/superscripts

eff	Effective (molecular + turbulent).
ESR	Electro slag remelting.
ϵ	Turbulent dissipation rate.
k	Turbulent kinetic energy.
liq	Liquidus / liquid.
p	Pulling (movement of the solid).
sol	Solidus.
UDF	User-defined function.
UDM	User-defined memory.
VAR	Vacuum arc remelting.
x	X-direction.
y	Y-direction.
z	Z-direction.

INTRODUCTION

Metallurgical processes are often modeled to obtain details of the inner fluid flow or temperature distribution, due to the difficult observation possibilities with classical measurement methods. The modelling of solidification processes is in focus of research since the 1970s (Erickson, 1975).

One of the common simulation programs ANSYS Fluent uses the enthalpy-porosity approach (ANSYS Inc., Release 14.5, 2012) which was introduced by Poirier (1987). ANSYS Fluent uses the assumption that the liquid fraction is proportional to the temperature in the solidification range. For many standard steels, this assumption will be an appropriate approach. In case of some nickel based superalloys, like alloy 718, the supposition is far-out the real material behavior.

Therefore, user-defined functions implement the solidification to reproduce the real material behavior.

SOLIDIFICATION PHENOMENA

Important for the simulation of solidification processes are the damping of the fluid flow in the mushy region and the solidification enthalpy. The damping is adjustable with the material specific mushy zone constant (Voller et al., 1990) and considers the liquid fraction also.

Figure 1 shows the liquid fraction of an alloy 718 in respect to the temperature in the solidification range calculated by JMatPro. Obviously, the linear approximation made by ANSYS Fluent is not appropriate for this material. After a cooling of 25 % of the temperature range the liquid fraction is not 75 % but only 40 %. Therefore, the

damping of the fluid flow is underestimated by ANSYS Fluent.

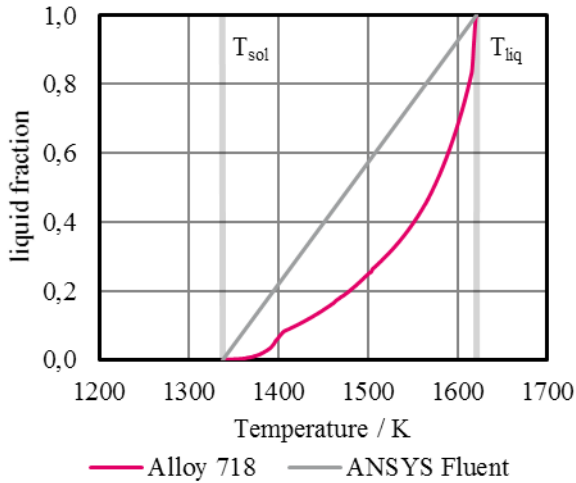


Figure 1: Liquid fraction of alloy 718 (Giesselmann et al., 2015) in comparison to ANSYS Fluent

The deviation of the liquid fraction from alloy 718 results in a nonlinear behavior of the enthalpy in the solidification range, because the solidification enthalpy is dependent on the liquid fraction.

Figure 2 shows the comparison of solidification enthalpies in respect to the temperature in the solidification range. The grey line shows the linear implementation of ANSYS Fluent. Obviously, the change in enthalpy of the mild steel (Koric and Thomas, 2008) is close to the approximation from ANSYS Fluent. Whereas, the red line, representing Alloy 718 (Overfelt et al., 1994), shows a considerably different behavior.

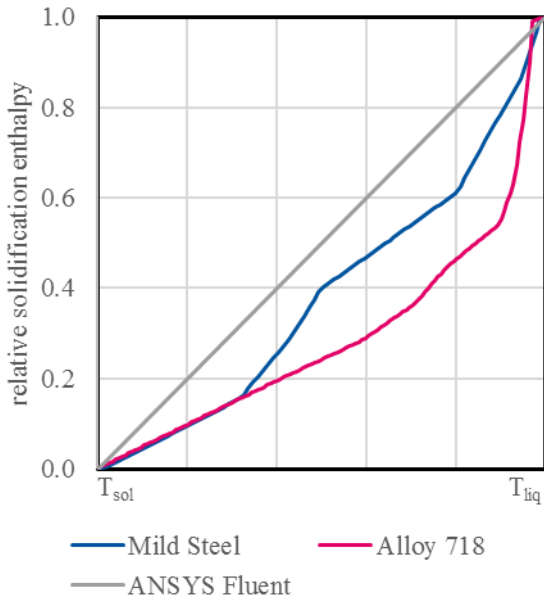


Figure 2: Comparison of solidification enthalpies (Overfelt et al., 1994, Koric and Thomas, 2008)

BUILT-IN SOLIDIFICATION IN ANSYS FLUENT

The solidification module from ANSYS Inc. (Release 14.5, 2012) uses the enthalpy-porosity approach to implement the damping of the fluid flow in the mushy region. Poirier (1987) shows, that the inter dendritic flow follows Darcy's law (Darcy, 1856):

Darcy's law

$$\nabla p = -\frac{\mu_D}{K} \cdot \mathbf{v} \quad (1)$$

Voller and Prakash (1987) implemented the awareness of Poirier (1987) in the fluid flow modeling. Later, a mushy zone constant was introduced to replace the dynamic viscosity μ_D and the unknown permeability K (Voller et al., 1990). The liquid fraction f_{liq} represents the change in permeability, whereas the mushy zone constant A_{mush} implements the different material behavior (2). The small number ϵ is equal 0.001 to avoid a division by zero (ANSYS Inc., Release 14.5, 2012).

$$\frac{\mu_D}{K} = \frac{(1 - f_{liq})^2}{f_{liq}^3 - l} \cdot A_{mush} \quad (2)$$

The ratio between viscosity and permeability (see formula (2)) is then inserted in the equations (3) and (4) to formulate the force F against the fluid flow \mathbf{v} as well as the momentum S against the turbulence quantities Φ .

$$\mathbf{F} = \frac{(1 - f_{liq})^2}{f_{liq}^3 - \epsilon} \cdot A_{mush} \cdot (\mathbf{v} - \mathbf{v}_p) \quad (3)$$

$$S = \frac{(1 - f_{liq})^2}{f_{liq}^3 - \epsilon} \cdot A_{mush} \cdot \Phi \quad (4)$$

The necessary turbulence quantities depend on the used turbulence model. Equation (4) is equal for all quantities like turbulent dissipation rate ϵ , turbulent kinetic energy k , specific dissipation ω and so on (ANSYS Inc., Release 14.5, 2012).

To show the implementation of the formula above, the momentum equation of the solver (5) is given below. The damping force F of the fluid flow (Equation (4)) is inserted in the last term.

$$\frac{\partial}{\partial t} (\rho \cdot \mathbf{v}) + \nabla \cdot (\rho \cdot \mathbf{v} \cdot \mathbf{v}) = -\nabla p + \nabla \cdot (\boldsymbol{\tau}) + \rho \cdot \mathbf{g} + \mathbf{F} \quad (5)$$

As mentioned in the previous chapter, the solidification enthalpy is distributed linear over the temperature range of solidification and implemented as source term S_m in the energy equation (6).

$$\frac{\partial}{\partial t} (\rho \cdot e) + \nabla \cdot (\mathbf{v} \cdot (\rho \cdot e + p)) = \nabla \cdot (\lambda_{eff} \cdot \nabla T + \boldsymbol{\tau}_{eff} \cdot \mathbf{v}) + Q_e \quad (6)$$

USER-DEFINED SOLIDIFICATION MODEL

To reconstruct the real material behavior of alloy 718 an in-house developed solidification model based on UDFs is used for several process models, like electro slag remelting (ESR) and vacuum arc remelting (VAR).

Approach

The aim of the modified solidification model is to implement the nonlinear behavior of the liquid fraction in respect to the temperature. The curve progression can be received for example from a Scheil-Gulliver approach like in Figure 1 or other calculation programs for thermo-physical data.

The idea was to reconstruct the solidification model of ANSYS Fluent by user-defined functions. Therefore, the main equations ((3) and (4)) for the damping are also used.

The solidification enthalpy is included in the heat capacity of the material.

Implementation

The implementation of the modified solidification model is based on a DEFINE_ADJUST function for the liquid fraction and several DEFINE_SOURCE functions for the damping. A modified heat capacity includes the change in enthalpy.

The liquid fraction should be adjusted very detailed to represent the real fluid flow. Therefore, liquid fraction and solidification enthalpy out of the thermophysical database are divided in 1 K steps.

Damping of the fluid flow

A DEFINE_ADJUST UDF loops over all the cells in the fluid regions to get the temperature of the cells. A look-up function searches the corresponding liquid fraction for these temperatures out of the tabulated liquid fractions. The liquid fraction is saved in a user-defined memory (UDM) for post processing.

Analog to the calculation procedure in ANSYS Fluent the ratio between viscosity and permeability is calculated with equation (2) and saved in another UDM. This ratio is the damping term of velocities and turbulence quantities (see equation (3) and (4)).

The damping force and momentum values are calculated in several DEFINE_SOURCE UDFs. One UDF for each velocity direction and the turbulence quantities, typical turbulent dissipation rate ϵ and turbulent kinetic energy k . The source value is the negative product of the damping term with the velocity or turbulence value (See equations (7) to (11)). If a pull velocity v_p moves the solid region, it has to be subtracted from the fluid velocity, here in the x direction:

$$F_x = -\frac{(1 - f_{liq})^2}{f_{liq}^3 - \epsilon} \cdot A_{mush} \cdot (v_x - v_p) \quad (7)$$

$$F_y = -\frac{(1 - f_{liq})^2}{f_{liq}^3 - \epsilon} \cdot A_{mush} \cdot v_y \quad (8)$$

$$F_z = -\frac{(1 - f_{liq})^2}{f_{liq}^3 - \epsilon} \cdot A_{mush} \cdot v_z \quad (9)$$

$$S_k = -\frac{(1 - f_{liq})^2}{f_{liq}^3 - \epsilon} \cdot A_{mush} \cdot k \quad (10)$$

$$S_\epsilon = -\frac{(1 - f_{liq})^2}{f_{liq}^3 - \epsilon} \cdot A_{mush} \cdot \epsilon \quad (11)$$

The five source terms have to be included for the corresponding values in the ANSYS Fluent interface. The program implements the source terms in the momentum equation (5) as well as the turbulence model.

Solidification enthalpy

To implement the nonlinear behavior of the solidification enthalpy (see Figure 2) the enthalpy is included in the heat capacity of the material (see Figure 3). Therefore, it is not necessary to modify the energy equation (6) of the solver.

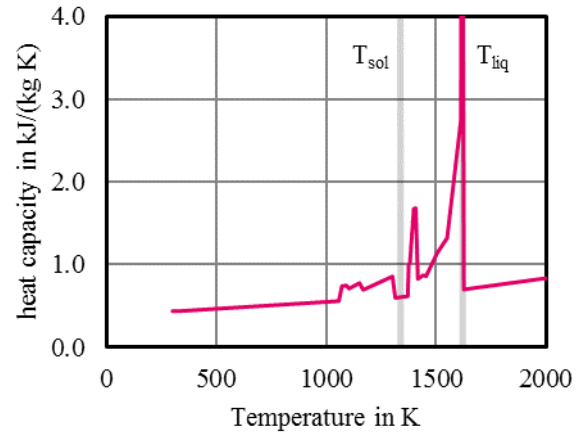


Figure 3: Heat capacity of alloy 718 including the solidification enthalpy (Giesselmann, 2014)

Obviously, most of the solidification enthalpy is needed or set free near to the liquidus temperature. This refers to the steep slope of the liquidus fraction in this area (compare Figure 1).

Another possibility to implement the enthalpy of solidification would be a DEFINE_SOURCE UDF. The advantage of the presented solution is the reversible character of the heat capacity. Because some parts of the simulated region maybe melt on again, the solution with source term would be more elaborate. Whereas the heat capacity offers directly the possibility for change of sign in the temperature derivation.

COMPARISON OF THE MODELS

To compare the built-in solidification of ANSYS Fluent with the UDF based solidification model a test case was set up. Figure 4 and Figure 5 show the flow of hot metal through a cooled pipe. The left face is a velocity inlet of hot liquid metal. The top wall is at constant temperature, which is lower than the solidus temperature. At the right side, the boundary is an outflow. The contour plot visualizes the liquid fraction from one (white) to zero (black). The black line symbolizes the position of 1 % solid fraction. The vectors and their lengths show the velocity. In Figure 4 the solidification model of ANSYS Fluent was used. Therefore, the liquid fraction increases uniformly over the whole solidification range.

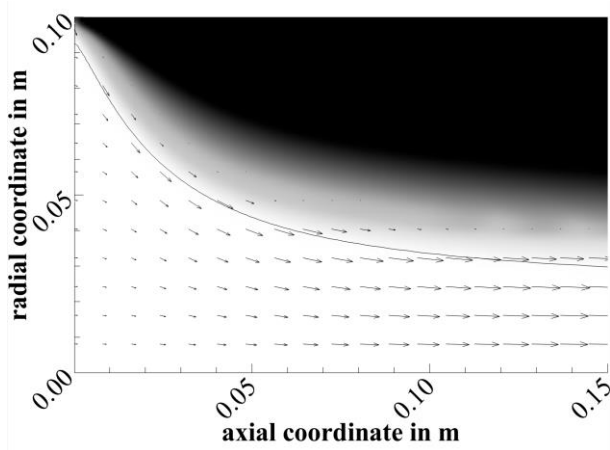


Figure 4: Test case: Built-in Fluent solidification model

Figure 5 shows the same test case simulation as Figure 4 with the UDF based solidification model. Obviously, the shape of the solidified area is slightly different, but more interesting is the case that there is sharp edge in the middle of the gray scale. Therefore, the fluid flow is damped at this position abruptly.

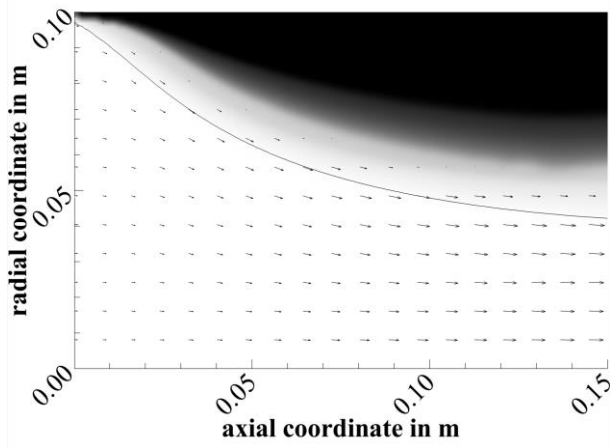


Figure 5: Test case: UDF solidification model

The comparison of the two test cases show the similarity of the models as well as the decisive differences. Whereas the flow in first case is damped smoothly, the damping with the UDF based model is more abrupt.

CONCLUSION

A modified solidification model for ANSYS Fluent was introduced. It offers the possibility to reproduce the real material behavior in context of liquid fraction in respect to temperature. Which is important for the damping of the fluid flow in the mushy region as well as the distribution of the solidification enthalpy over temperature.

The solidification model of ANSYS Fluent was modified and calculated in a user-defined function to adjust the liquid fraction concerning the cell temperature properly. The damping of the motion values is then implemented by source terms for velocities and turbulence quantities. The solidification enthalpy is included in the heat capacity of the material. Therefore, the enthalpy can be fitted very detailed.

A test case shows the similarities and differences of the two models. The modified solidification implements a more abrupt damping of the fluid flow.

The modified solidification model is able to replicate the material behavior more detailed than the built-in solidification module of ANSYS Fluent.

REFERENCES

ANSYS INC., (Release 14.5, 2012), "ANSYS® Academic Research Help System".

DARCY, H.P.G., (1856), "Dètermination des lois d'écoulement de l'eau à travers le sable".

ERICKSON, W.C., (1975), "Use of a general-purpose heat-transfer code for casting simulation", United States.

GIESSELMANN, N., (2014), "Numerische Untersuchungen des Elektroschlack-Umschmelzprozesses für Alloy 718", Dissertation, Aachen, RWTH Aachen University, Fakultät für Georesourcen und Materialtechnik, 140.

GIESSELMANN, N., et al., (2015), "Coupling of Multiple Numerical Models to Simulate Electroslag Remelting Process for Alloy 718", *ISIJ International*, **55**, 1408-1415.

KORIC, S. and THOMAS, B.G., (2008), "Thermo-mechanical models of steel solidification based on two elastic visco-plastic constitutive laws", *Journal of Materials Processing Technology*, **197**, 408-418.

OVERFELT, R.A., et al., (1994), "Porosity in cast equiaxed alloy 718", *International Symposium on Superalloys 718, 625, 706 and Various Derivatives*, Pittsburgh, 189-200.

POIRIER, D., (1987), "Permeability for flow of interdendritic liquid in columnar-dendritic alloys", *Metallurgical and Materials Transactions B*, **18**, 245-255.

VOLLER, V.R., et al., (1990), "Modelling the mushy region in a binary alloy", *Applied Mathematical Modelling*, **14**, 320-326.

VOLLER, V.R. and PRAKASH, C., (1987), "A fixed grid numerical modelling methodology for convection-diffusion mushy region phase-change problems", *International Journal of Heat and Mass Transfer*, **30**, 1709-1719.